PERGAMON

International Journal of Heat and Mass Transfer 41 (1998) 3099–3108

International Journal of HEAT and MASS TRANSFER

A guarded cold plate apparatus for absolute measurement of heat flow

C. J. Dey[a], A. J. Read[a], R. E. Collins[a,*], M. Brunotte[b]

[a] *School of Physics, The University of Sydney, N.S.W., 2006, Australia*
[b] *Schott-Rohrglas GmbH, Postfach 1180, D-95660 Mitterteich, Germany*

Received 14 April 1997; in final form 27 December 1997

Abstract

This paper describes the working principles and operation of a new instrument for making absolute measurements of heat flow. This instrument, called the guarded cold plate apparatus, differs from standard guarded hot plate designs in that the measured heat flow through the sample is towards the metering side, rather than away from it. A guarded cold plate apparatus is described for measurement of the radiative heat flow from high emittance surfaces at temperatures up to 200°C. Values of emittance obtained from such measurements agree with those derived from infrared reflectance data to within ±5%.

Nomenclature

A surface area
E black body spectrum
q rate of radiative heat transfer
T temperature.

Greek symbols

Δ difference
ε emittance
θ angle to normal
λ wavelength
σ Stefan–Boltzmann constant.

Subscripts

g guard
link thermal link
mp metering piece
s sample
1, 2 denote surfaces for heat transfer.

1. Introduction

The guarded hot plate apparatus is used widely for the accurate measurement of heat flow, particularly through thermally insulating materials [1]. Figure 1(a) shows a schematic diagram of the measurement principle of this type of device. A thermal conductor, called the metering piece in this paper, is placed in good thermal contact with one side of the sample under test. The metering piece is surrounded by a guard region which is also in good thermal contact with the sample. The temperature of the guard, and therefore of the side of the sample with which it is in contact, is held constant. The other side of the sample is held at a lower temperature. Heat therefore flows from the guard directly into the sample. Heat also flows from the guard to the metering piece, and then into the sample. The temperature of the metering piece is thus slightly lower than that of the guard. To a first approximation, the temperature difference between the metering piece and the guard is proportional to the rate of heat flow through the sample. An elegant null detection method can be used to obtain an absolute measurement of this heat flow. Power is dissipated in a resistive heater embedded in the metering piece, thus increasing its temperature. When the temperature of the metering piece is exactly equal to that of the guard, all of this resistive

* Corresponding author. Tel.: 00 61 2 9351 2537; fax: 00 61 2 9351; e-mail: r.collins@physics.usyd.edu.au.

0017–9310/98 $19.00
PII: S0017-9310(98)00026-X

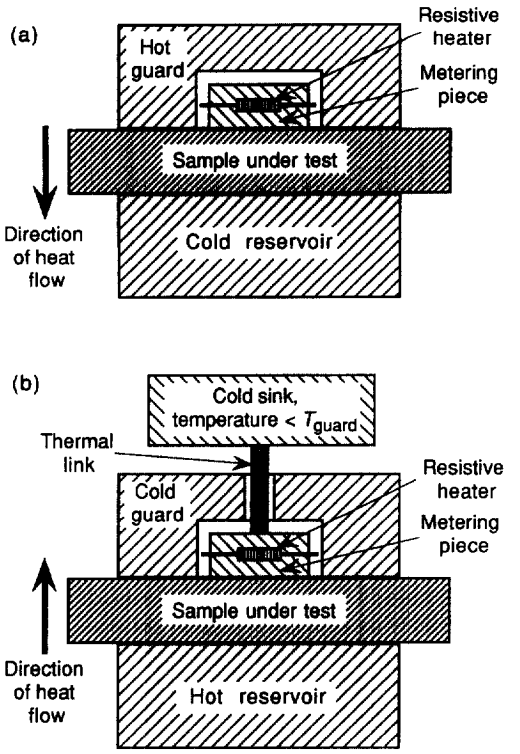

Fig. 1. Schematic diagrams illustrating the principles of operation of: (a) the guarded hot plate apparatus; and (b) the guarded cold plate apparatus.

power flows through the sample. A measurement of the power under this null conditions thus enables the heat flow through the sample to be determined. For high accuracy measurements in practical designs of guarded hot plates, it is of course necessary to ensure that parasitic heat flows from the metering piece are negligible and that the measurement area is defined precisely [2].

Intrinsic to the design of guarded hot plates is that, as the name implies, the guarded metering piece is on the hot side of the sample. In this type of apparatus, this is unavoidable because it is only possible to add heat to the metering piece by dissipation of resistive power. This means that the structure of the metering piece and the guard, including their temperature sensors and associated electronics, must be designed to withstand the upper temperature limit at which it is desired to make measurements [3]. At high temperatures, it is quite difficult to achieve high sensitivity in the detection of the null, and to reduce parasitic heat flows to low levels.

This paper describes the design and construction of a guarded cold plate apparatus in which a null method is used to measure heat flow into a metering piece. The principle of the guarded cold plate technique is shown in Fig. 1(b). As before, the metering piece is surrounded by a guard at constant temperature and both the metering piece and the guard are placed in good thermal contact with the sample. In this case, however, the metering part of the apparatus is on the lower temperature side of the sample. The metering piece is also connected by a thermal link to a second cold region, the temperature of which is slightly less than that of the guard. In this paper, we use the term cold sink to describe the second cold region. Initially, the condition for equality of the temperatures of the metering piece and guard is established by setting the temperatures of the guard, the cold plate and the cold sink to be precisely equal. The temperature of the cold sink is then reduced, and heat flow is established from the metering piece through the thermal link to the cold sink. Under these conditions, the temperature of the metering piece is slightly less than that of the guard by an amount depending on the various thermal impedances between the metering piece and the guard, the cold sink, and the sample. Resistive power is then dissipated in the metering piece, raising its temperature to be precisely equal to that of the guard. We call this the primary null condition. All of this resistive power flows along the thermal link to the cold sink; none flows through the sample since, under these conditions, there is no temperature difference across the sample. A temperature difference is then established across the sample, and heat flow occurs through the sample to the metering piece, increasing its temperature. The power in the resistor is then reduced, decreasing the temperature of the metering piece until it is again equal to that of the guard. We call this condition the secondary null. The amount of heat flowing from the sample to the metering piece is the difference between the levels of power dissipation in the resistor under the primary and secondary null conditions.

It will be appreciated that, like the guarded hot plate, the guarded cold plate is also a true null instrument. It is not necessary to know accurately the temperature of the second cold bath, nor the thermal impedances within the apparatus. It is also unnecessary to measure precisely the temperature difference between the metering piece and the guard. All that is required is detection of the condition of equality of these temperatures. In fact, both instruments require the detection of two null conditions: at zero heat flow through the sample (the primary null), and with heat flowing through the sample (the secondary null). Compared to a guarded hot plate, the only additional experimental constraint is that the total heat flow between the metering piece and the cold sink should remain constant during a measurement procedure.

The term 'guarded cold plate' has previously been applied to other instruments for the measurement of heat flow. For example, Shewen et al. [4] have described an instrument which uses the Peltier effect to remove heat from its metering section. Thermoelectric modules were embedded in a metallic plate and, depending on the direction of the imposed current, heat could be liberated or

absorbed at the metering piece. The operating principle of this device was therefore very similar to that of the present guarded cold plate, and it can be regarded as a null instrument. In order to determine the magnitude of the power which was removed from the metering piece, however, it was necessary to undertake a complex calibration procedure to account for the effects of Peltier and resistive heat flows, and for the influence of various thermal resistances at the heating and cooling junctions of the Peltier devices.

Mention should be made of another instrument in the literature, which has also been termed a guarded cold plate [5], and which was designed to measure heat transfer through multi-layer superinsulations at low temperatures. In this instrument, the guard was maintained at very low temperatures using a cryogenic fluid, and the other side of the sample was heated. The rate of heat flow through the sample was then determined by measuring the rate of boil-off of cryogenic fluid in the metering vessel. This is an example of a general class of measurement instrument in which heat flows into a measuring region. Virtually all radiation detectors also operate in this way [6]. The specific additional feature which distinguishes the guard cold plate instrument described here is the combination of thermal guarding and null detection.

In this paper, we described the design, construction and performance of a guarded cold plate apparatus which was developed specifically to measure radiative heat flow from the evacuated surface of small area (~ 2 cm^2) samples. The principles of operation are applicable to samples of any area, however, and to the measurement of heat transfer by any physical mechanism.

2. Design principles and construction

Some of the design features of this apparatus are specifically determined by its particular application—to make accurate measurements of radiative heat transfer. These include the need for the instrument to operate in a vacuum environment, and the necessity for the front surface to have a very high emittance (high infrared absorbance). Other aspects of the design would be important for all guarded cold plate instruments: for example, a method must be used to achieve a stable, controllable extraction of heat from the metering piece. In this section, we present details of the design and construction of this guarded cold plate apparatus. Wherever possible, the discussion concentrates on features which are of generic significance.

2.1. Mechanical and thermal design

Figure 2 is a diagram of the metering piece and guard of the guarded cold plate apparatus showing the method of construction. The most critical part of the guarded cold plate apparatus is the metering piece. This component is machined from copper in order to minimise internal temperature gradients. The front, evacuated face of the metering piece is circular, with diameter 15.2 mm, and is mounted planar with the front surface of the guard, and separated from it by a narrow (0.05 mm) annular gap. The accurate location of the metering piece relative to the guard is achieved with an annular stainless steel disk which, through O-rings (not shown in Fig. 2), also provides the vacuum seal between these two components. The stainless steel disk is the dominant thermal impedance between the metering piece and guard. It is essential that this impedance be as large as possible since it determines the magnitude of the temperature difference through which the null condition is detected. Both metering piece and guard are therefore tapered away from their front-surface diameters, in order to increase the annular dimension of the disk.

The metering piece extends axially beyond the stainless steel disk in order to provide space for mounting a resistor that provides electrical heating. The far end of the metering piece is connected by a cylindrical stainless steel rod (the thermal link) to a second reservoir (the cold sink) which is maintained at a lower temperature than the guard. This establishes stable and well defined heat removal from the metering piece.

The temperatures of the guard, and of the cold sink, are determined by water which circulates through insulated pipes from separate temperature-controlled baths. Temperatures in the water lines are measured near each inlet and outlet with a platinum resistance thermometer inserted into re-entrant pockets. The temperatures of each water stream are stable to ± 0.01°C. The front part of the guard is machined from copper in order to minimise temperature gradients.

The water flow through the guard is split into two streams. About two-thirds of the flow is close to the front surface of the guard, and the rest is also parallel to this surface, but displaced some distance from it. The first stream serves to define the temperature of the front surface of the guard and, specifically, the temperature at the outer diameter of the stainless steel disk. The second stream achieves two functions. It provides a stable temperature for the hot end of a co-axial brass tube that surrounds the thermal link. This tube acts as a thermal shield by establishing well-defined boundary conditions around the link, thus resulting in constant heat flow to the cold sink. The second water stream also creates a temperature-stabilised cavity which contains the electronics used for detection of the null condition. The rate of the water flow to the metering piece ~ 0.06 l s^{-1}. This results in large heat transfer coefficients (~ 3000 W m^{-2} K^{-1}) at the internal surfaces. Systematic errors associated with the small temperature drop across the water–surface interface in the guard are discussed below. The

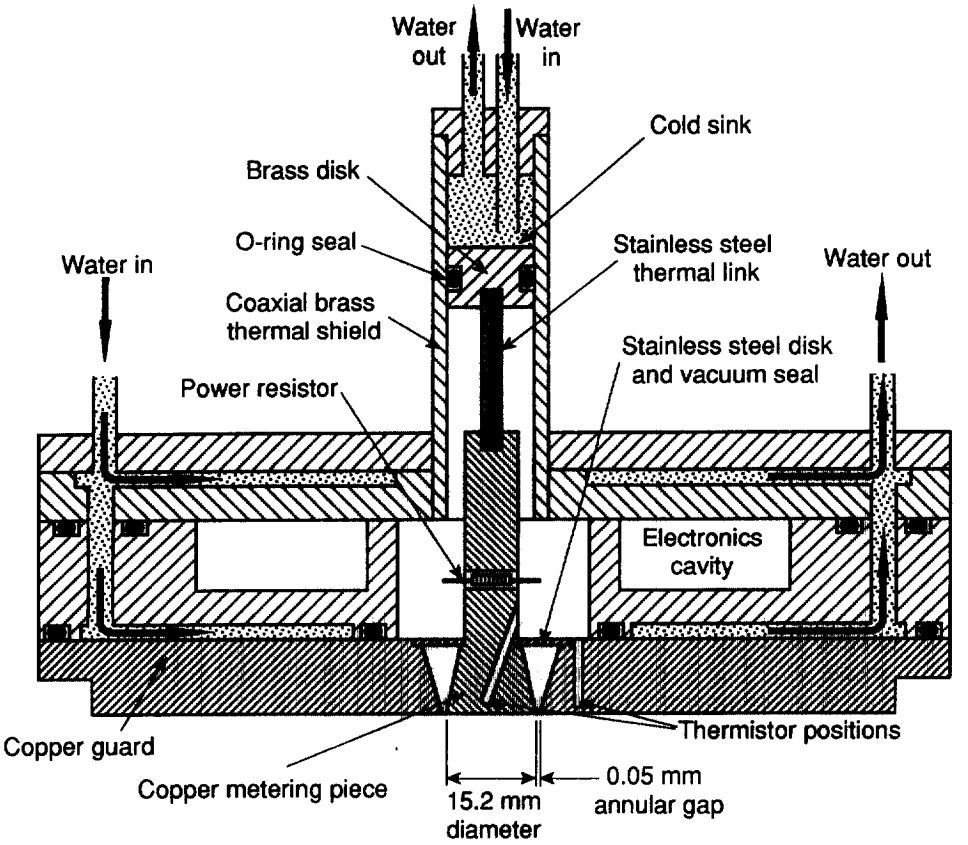

Fig. 2. Constructional details of the guarded cold plate apparatus.

water flow into the cold sink is designed to achieve a very high heat transfer coefficient at the surface of a brass disk attached to the end of the thermal link, resulting in negligible temperature drop across this interface.

The instrument was designed to operate with the guard at the same temperature as the air conditioned laboratory. Experience with a very high accuracy, small area guarded hot plate [2] has shown that this leads to the most stable operation, and results in very small parasitic heat flows from the metering piece.

The dimensions of the stainless steel thermal link (15 mm long and 4.75 mm diameter) were chosen so that the instrument can measure radiative heat flows from high emittance surfaces at temperatures up to $\sim 200^{\circ}C$, for a temperature difference of $20^{\circ}C$ across the link.

The performance of any guarded heat flow measurement instrument is critically dependent on the accuracy of detection of the null condition when the temperature of the metering piece is precisely equal to that of the guard. In this guarded cold plate apparatus, the metering piece and guard are in reasonably good thermal contact through the stainless steel disk. High accuracy measurements therefore require the detection of very small temperature differences ($\sim 10^{-4}$ K) between these components. This is achieved using high resistance thermistors which are embedded in holes in each component in a way which ensures very good thermal contact. The thermistors are connected by very thin wires to a Wheatstone bridge and high stability amplifier which are located in the temperature stabilised cavity. Parasitic heat flows along these wires (and also along those to the resistor) are reduced to negligible levels by careful thermal termination [2].

It is noted that the accuracy, calibration, and matching of the temperature sensors in the metering piece and guard are unimportant for satisfactory operation of the instrument, since all measurements are made at the null condition when these two temperatures are precisely equal. As noted in Section 1, in the set-up procedure of the apparatus this condition of temperature equality is established by determining the zero of the bridge whilst operating the instrument with all components (guard,

cold sink, and sample) at the same temperature. All subsequent measurements are made with the guard at the same temperature as during the identification of this zero condition. The primary and secondary null conditions, when the temperatures of the metering piece and guard are equal, are then determined by establishing the same value of the bridge output as for the measurement of the zero condition.

2.2. Measurement of radiative heat flow

As noted above, this paper is primarily concerned with describing the general principles of the guarded cold plate instrument which may be applied to the measurement of heat flow through any type of insulating material. The particular guarded cold plate instrument that has been built incorporates several features which are of specific relevance to the measurement of radiative heat flow. For example, it is essential to evacuate the region adjacent to the metering piece and guard. The mounting configuration of the metering piece must therefore provide an adequate leak-free seal, and must be capable of withstanding the pressure differential associated with this vacuum.

Figure 3 shows details of the construction of the vacuum chamber, including the method of mounting the guarded cold plate apparatus and the sample. The space between the sample and the measuring apparatus is evacuated to a pressure below 10^{-2} Pa using a turbomolecular pump. At this pressure, gaseous conduction is negligible relative to radiative heat flow.

The position of the hot surface can be adjusted from outside the vacuum chamber. This surface is normally separated from the metering piece and guard by a parallel evacuated gap of ~ 0.5 mm. This corresponds to a radiation shape factor for net energy exchange of greater than 0.999. The temperature of this test surface is defined either by circulating temperature-controlled water (not shown in Fig. 3) or, at high temperatures, by dissipating power in a cartridge heater.

It is well known that the rate of radiative heat flow between two surfaces depends on the infrared optical properties of both surfaces. For plane parallel surfaces of hemispherical emissivities ε_1 and ε_2, at temperatures T_1 and T_2, the rate of the radiative heat transfer through area A is conventionally written:

$$q_{\text{radiation}} = \varepsilon_{\text{effective}} \sigma A (T_1^4 - T_2^4) \tag{1}$$

where σ is the Stefan–Boltzmann constant, and $\varepsilon_{\text{effective}}$ is the effective emittance for radiative heat flow between the combination of surfaces, defined as:

$$\frac{1}{\varepsilon_{\text{effective}}} = \frac{1}{\varepsilon_1} + \frac{1}{\varepsilon_2} - 1. \tag{2}$$

It is well known that these relationships are valid only for surfaces that are grey (that is for which the infrared reflectance is independent of wavelength over the relevant range of thermal wavelengths). For non-grey surfaces, equations (1) and (2) may results in significant errors. For example, Zhang et al. [7] have shown that these relations underestimate the radiative heat flow between uncoated soda lime glass surfaces by about 4%. An exact calculation of radiative heat flow between plane, parallel, specularly reflecting surfaces of area A involves a simultaneous integral over wavelength λ and angle to the normal θ, of the black body spectrum $E(\lambda, T)$ at the temperatures of the surfaces T_1 and T_2, weighted by the combined emittances of the surfaces, calculated in a way similar to equation (2), at each angle and wavelength:

$$q_{\text{radiation}} = A \int_0^{\pi/2} \sin 2\theta \, \mathrm{d}\theta \times \int_0^{\infty} \frac{E(\lambda, T_1) - E(\lambda, T_2)}{\dfrac{1}{\varepsilon_1(\lambda, \theta, T_1)} + \dfrac{1}{\varepsilon_2(\lambda, \theta, T_2)} - 1} \mathrm{d}\lambda. \tag{3}$$

Despite these complexities, equations (1) and (2) give an exact value for radiative heat flow when one of the surfaces is black ($\varepsilon = 1$). In this case, the effective emittance is simply the hemispherical emittance of the other surface. In the guarded cold plate instrument, it is therefore highly desirable to make the evacuated surface of the metering piece with a very high emittance in order that the rate of radiative heat transfer should be primarily dependent on the emittance of the surface under test. The normal method of achieving a very high emittance is to construct a large cavity with a very small aperture. It was not possible to incorporate such a structure into the guarded cold plate, as the metering piece is part of a plane, parallel surface. Several metering pieces were built with different designs of absorbing surfaces. A full description of these surfaces, and of their performance, is given elsewhere [8]. In this paper, the data presented were obtained with a metering piece which has a front surface consisting of a large number of small, thin walled copper tubes. The tubes are 5 mm long, 1.6 m in diameter, and have a wall thickness of 0.4 mm. Because of the comparatively large wall thickness, the outer ends of the tubes are machined to a wall thickness of ~ 0.1 mm. The tubes are soft soldered at the inner ends into a cavity in the metering piece in order to achieve good thermal contact. All of the exposed surfaces of the tubes were coated with black paint having a thermal emittance of 0.89 ± 0.01. As will be seen, this design results in a useful increase of the emittance that was obtained compared to that of the black paint.

3. Systematic errors

The operating principle of the guarded cold plate apparatus is based on the assumption that some of the

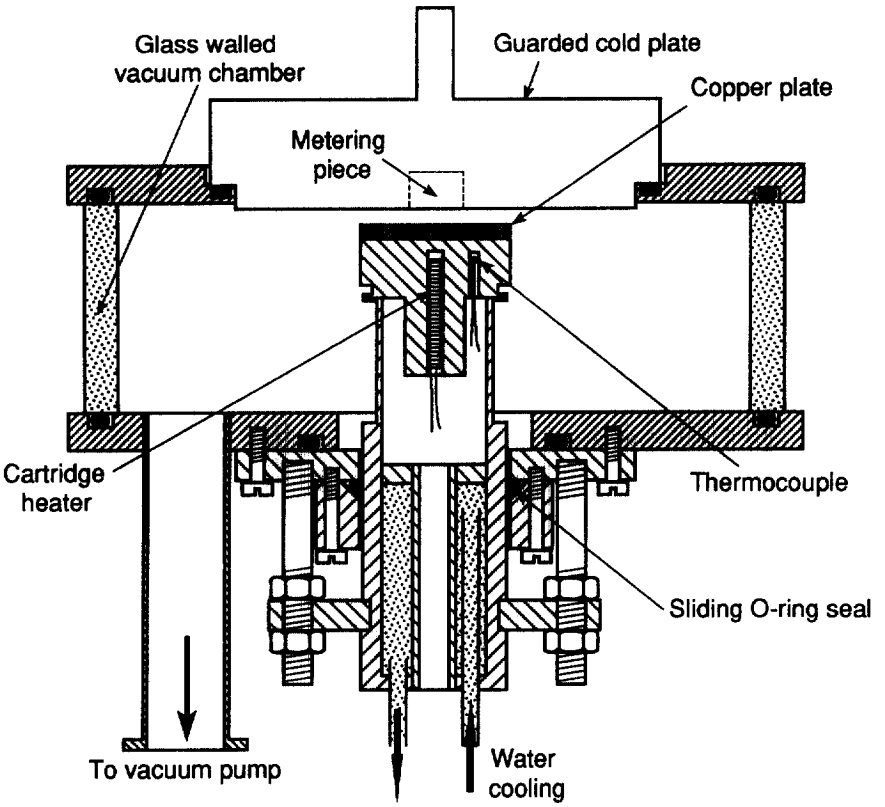

Fig. 3. Details of the construction of the vacuum chamber, showing relative positions and mounting arrangements of the guarded cold plate apparatus and the sample.

heat which flows from the metering piece to the cold sink under the primary null condition is exactly replaced by heat flow from the external source to the metering piece under the secondary null condition. On the basis of this assumption, the heat flow from the sample is equal to the difference in the power dissipated in the resistive heater in the metering piece under these two null conditions. In the actual instrument, there are several effects which result in small departures from this ideal behaviour. Firstly, the temperature distribution in the metering piece, and the thermal impedance through which heat flows in the metering piece, both change slightly between the primary and secondary null conditions. This results in small differences in the heat flow to the cold sink between these two conditions. Secondly, both null conditions, where the measured temperature difference between the thermistors in the metering piece and the guard is zero, are assumed to correspond exactly to zero temperature difference across the dominant thermal impedance between these two components: the stainless steel disk. This only holds precisely at the primary null, where there is no heat flow in the vicinity of this component; at the secondary null, small temperature gradients exist in the metering piece and guard close to the stainless steel disk. This causes additional heat to be injected into the metering piece which is not present at the primary null. The first of these two sources of systematic error is specific to the guarded cold plate. The second could also occur in convectional guarded hot plate designs.

The raw heat flow data can be corrected by adjusting the readings for any net change in heat flow to the cold sink, or in the stainless steel disk, due to these systematic departures from ideal operation at the secondary null. In order to do this, it is necessary to obtain a detailed understanding of the temperature distributions within the apparatus, particularly in the region of the stainless steel disk and resistive heater. The system was therefore modelled using a commercial finite element package [9]. The finite element model is cylindrically symmetric, rather than three dimensional, but it contains all of the essential details necessary to determine the important features of the temperature distributions. Full details of the model, and the results obtained, are given elsewhere

[8]. In this paper, we present the conclusions drawn from the modelling results in a way which identifies the design features that contribute to systematic errors.

We begin by considering the temperature distribution in the instrument at the primary null condition where the temperatures of the sample and the guard are equal. In this case, the only heat flow is from the resistive heater to the cold sink, and significant temperature non-uniformities exist only in the thermal link, and in that part of the metering piece between the resistor and the thermal link. In this design, the thermal impedances of these two regions are 52 and 2 K W^{-1}, respectively. The rest of the metering piece, the stainless steel disk, and the guard are essentially isothermal. Their temperature is equal to that of the water circulating through the guard. The power dissipated in the resistive heater at the primary null is therefore determined by the temperature difference between the two circulating water streams, and the thermal impedance between the resistive heater and the cold sink.

At the secondary null condition, there is radiative heat flow into the metering piece and the guard at their front, evacuated faces. This results in a small temperature difference across the interface between the guard and the circulating water, and also in additional small, but significant temperature gradients in the metering piece and guard. The additional temperature difference across the guard–water interface increases the temperature of the stainless steel disk. This, in turn, increases the temperature difference across the thermal link, and thus causes a slight increase in the heat flow to the cold sink. Modelling results indicate that, in this apparatus, the increase is equal to 0.5% of the radiative heat flow into the metering piece.

A second effect caused by radiative heat flow entering the metering piece is associated with the location of the resistor in the metering piece, and causes a correction in the opposite sense. Ideally, the radiative heat which enters the evacuated surface of the metering piece replaces a precisely equal amount of heat generated in the resistor. However, the heat due to absorbed radiation must flow along an additional length of the metering piece between the stainless steel disk and the resistor. In this apparatus, the thermal impedance of this part of the metering piece is ~ 0.6 K W^{-1}. This results in a small additional temperature drop between the stainless steel disk and the cold sink which reduces the heat flow down the thermal link. The magnitude of this effect is 0.9% of the radiative heat which is absorbed at the evacuated surface of the metering piece. The combined influence of these two effects is to reduce the heat flow to the cold sink at the secondary null by $0.9-0.5=0.4\%$ of the absorbed radiative heat flow. This radiative flux is therefore less than the difference between the power at the primary and secondary nulls by this amount.

Both of these effects change the magnitude of the heat flow to the cold sink and, as noted, are therefore specific to the guarded cold plate apparatus. There is a third small correction which must be applied to the raw data that would also be needed in a guarded hot plate apparatus of similar geometry. This arises because of differences in the flow patterns of the absorbed radiative heat in the metering piece and guard between the front evacuated surfaces and the stainless steel disk. These differences give rise to a small temperature difference across the disk at the secondary null condition where the temperatures of the two thermistors are equal. In this apparatus, this results in an injection of heat into the metering piece at the disk equal to 0.5% of the absorbed radiative heat flow in the metering piece. The estimate of radiative heat flow obtained from the difference between the powers at the primary and secondary nulls must therefore be reduced by this amount. The total correction which must be applied to the raw data in this apparatus is thus a reduction of 0.9%.

Design strategies can be adopted which reduce systematic errors in the guarded cold plate apparatus. Firstly, the flow rate of the water which defines the guard temperature can be increased to reduce temperature drops across the water–guard interface which occur when external heat enters the guard. Secondly, this water should flow as close as possible to the dominant thermal impedance between metering piece and guard (the stainless steel disk) in order to minimise any change in the temperature of the guard side of this impedance when external heat flows. Thirdly, the heat source in the metering piece should be located in such a way that similar heat flow patterns occur in the metering piece under primary and secondary null conditions. Finally, and of relevance to all forms of guarded heat flow measuring instrument, the positions of the temperature sensors used to detect the null condition should be such that zero detected temperature difference corresponds precisely to zero actual temperature difference across the dominant thermal impedance between the metering piece and the guard.

Of course, practical design constraints, such as the requirement for a vacuum seal between the metering piece and the guard may, as in this apparatus, limit the degree to which these conditions can be met. It is important to understand the magnitude of the consequent systematic errors. It is therefore strongly recommended that any future design of a similar apparatus be based on detailed thermal modelling, such as that described here.

4. Results

The first step in the measurement procedure with the guarded cold plate apparatus is the establishment of the primary null condition, where no external heat flows into the metering piece and guard. This is achieved exper-

imentally by using a polished copper sample which has very low emittance, and setting the sample temperature to be as close as possible to that of the guard. Figure 4 shows data taken under such conditions: the temperature difference between the metering piece and the guard $T_{mp}-T_g$ is plotted as a function of resistive power dissipated in the metering piece for different values of the temperature difference across the thermal link ΔT_{link}. The linearity of each line reflects the near-constancy of the thermal impedance between the metering piece and the guard. The value for the impedance of 11.9 K W^{-1} obtained from the experimental data of Fig. 4 is in good agreement with the value of 12.2 K W^{-1} calculated from the parallel combination of the impedances of the stainless steel disk (20 K W^{-1}), between the metering piece and the cold sink (65 K W^{-1}), and between the metering piece and the guard through the air surrounding the metering piece (60 K W^{-1}).

At the primary null condition in Fig. 4 where the temperatures of the metering piece and guard are equal, all of the resistive power supplied to the metering piece flows to the cold sink. Figure 5 shows a plot of this power as a function of temperature difference between the guard and the cold sink ΔT_{link}. These data exhibit a nearly linear relationship and yield a thermal impedance of 74 K W^{-1} between the metering piece and cold sink. This is in reasonable agreement with the design value of 65 K W^{-1}. The slight departure from linearity is consistent with the 1.5% decrease in the thermal conductivity of stainless steel over the 10°C reduction of mean temperature of the thermal link for these data.

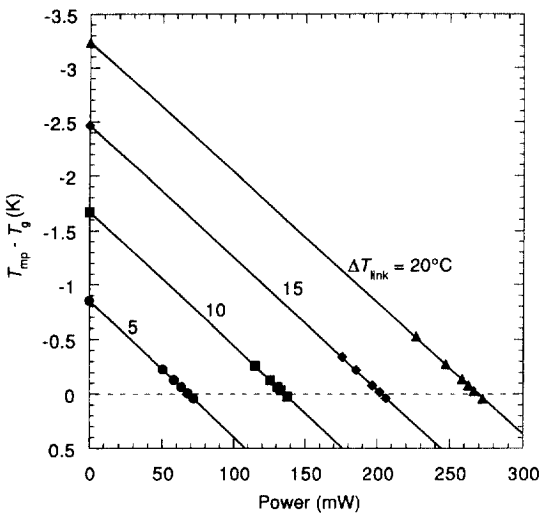

Fig. 4. Establishment of the primary null condition. Measured values of the difference in the temperatures of the metering piece and guard $T_{mp}-T_g$ are plotted as a function of the power dissipated in the metering piece resistor, for zero temperature difference between the guard and the sample surface. Data are shown for several values of the temperature difference across the thermal link ΔT_{link}.

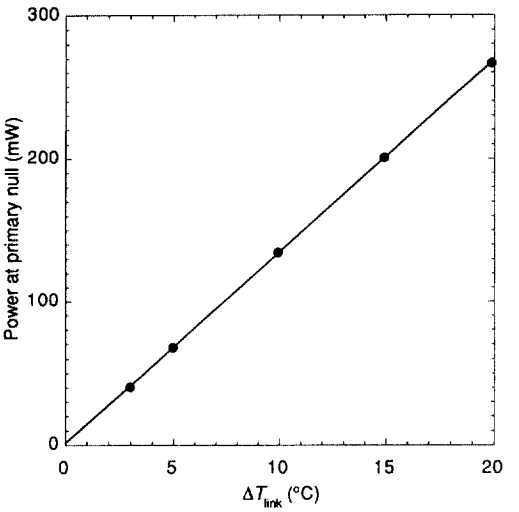

Fig. 5. Experimental measurements of the resistive power at the primary null condition as a function of the temperature difference across the thermal link ΔT_{link}.

The results of Fig. 5 calibrate the rate of heat removal from the metering piece and form the basis for the subsequent measurement of radiative heat flow entering it from the evacuated surface. In practice, the secondary null is established by maintaining the cold sink at a constant temperature, and recording the decrease of resistive power at null for an increase in the sample temperature. Figure 6 shows an example of such experimental data for radiative heat transfer between an uncoated soda-lime glass surface at temperature T_s and the tubed metering piece at temperature T_g.

Measurements of radiative heat flow q_s for uncoated glass, and for glass coated with pyrolytically deposited tin oxide coating (K glass [10]) are shown in Fig. 7. These data include the small corrections for systematic errors discussed in the previous section. The data in these figures are plotted against $T_1^4-T_2^4$, where the calculation of the surface temperature of the sample has included the temperature drop through the thickness of the glass. These data exhibit a dependence on temperature which is close to that given in equation (1). Small departures of the data from a linear relationship can be seen, however. These departures are attributable mostly to the temperature dependence of the emittance of the glass samples, and are more apparent in the following figure.

In this work, we have determined the emittance of the surfaces of the metering pieces by applying equations (1) and (2) to experimental measurements of radiative heat flow between identical surfaces. For flat black paint, and the tubed painted surface, these values of emittance are 0.89 ± 0.01 and 0.94 ± 0.01, respectively, at a temperature

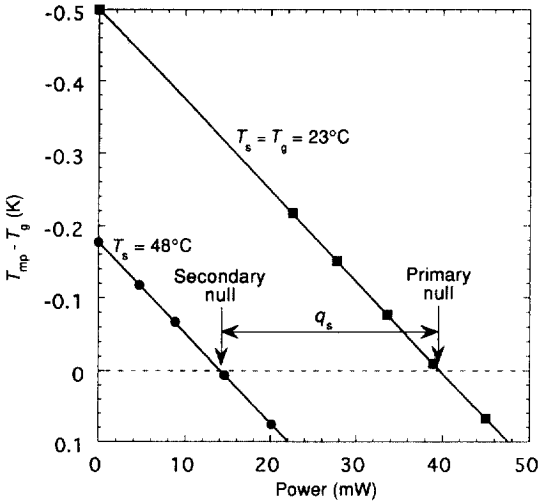

Fig. 6. Typical experimental data showing the primary and secondary null conditions for radiative heat transfer between an uncoated glass sample at temperatures $T_s = 23$ C and 48 C, and the tubed metering piece at temperature $T_g = 23$ C. The cold sink temperature was 20 C. The difference in resistive power between the two null conditions is a measure of the radiative heat flow from the sample q_s.

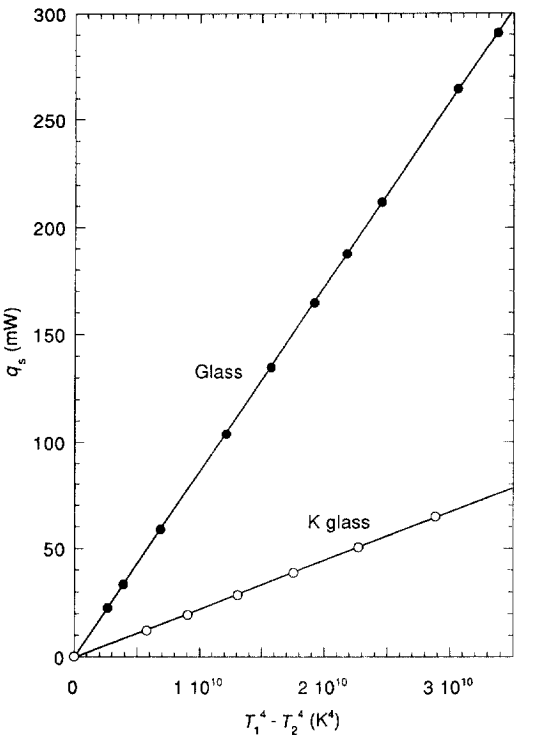

Fig. 7. Experimental guarded cold plate measurements of the radiative heat flow q_s to the tubed metering piece from uncoated glass, and glass coated with a pyrolytically deposited in tin oxide coating (K glass). the data are plotted against $T_1^4 - T_2^4$ and show slight departures from this form of temperature dependence. The temperatures of the hot surfaces are corrected for the temperature difference across the glass plates.

of 23 C. This value of emittance for the tubed surface can be used with equations (1) and (2) and the data of Fig. 7 to determine the temperature dependence of the emittance of the uncoated, and coated glass surfaces. Such results are shown in Fig. 8 together with values of hemispherical emittance calculated from infrared reflectance measurements [7, 11]. This calculation procedure is presented in more detail elsewhere [7].

There are two contributions to the uncertainties in the values of emittance shown in Fig. 8. Uncertainties in the detection of the null conditions, and in the measurement of the three temperatures in the guarded cold plate, give rise to errors which decrease with increasing sample temperature, and with increasing measured heat flow. In addition, as discussed in Section 2, there are systematic errors in the estimation of the heat flow due to the application of equations (1) and (2), rather than equation (3), although the magnitude of these errors is difficult to estimate in this case. However, for uncoated glass, it is likely that this error will be in the same sense as for the case of radiative heat flow between soda lime glass sheets; that is, that equations (1) and (2) will overestimate the magnitude of hemispherical emittances obtained from experimental data by a few percent. This effect may explain most of the systematic differences between the measured and calculated emittances of uncoated glass seen in Fig. 8.

This explanation does not account for the difference between the measured and modelled emittances for K glass since, for this combination of surfaces, equation (3) gives very similar results to those obtained with equations (1) and (2). However, the errors in the values of emittance of K glass obtained from infrared reflectance data have been shown to be about ± 0.005 [7]. When this additional error is included, the modelled hemispherical emittance data for K glass lie just within the error bars of the experimental results. It is also worth noting that the measured temperature dependencies of emittances agree with the modelling results, for both glass and K glass surfaces. Thus, to within experimental error of approximately $\pm 5\%$, there is agreement between the thermal and optical measurements.

5. Conclusion

A novel null instrument—the guarded cold plate apparatus—has been developed. This instrument provides accurate, absolute measurements of radiative heat flow towards, rather than away from the metering side, of the apparatus. In this guarded cold plate apparatus,

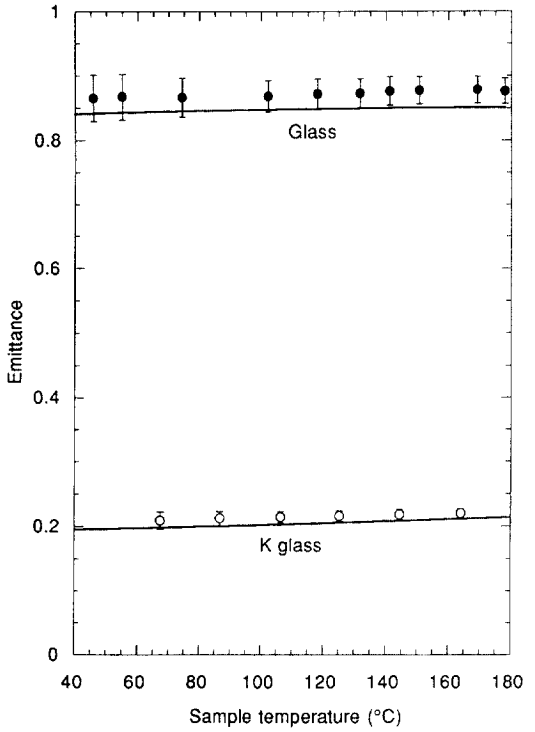

Fig. 8. Values of emittance for uncoated and K glass. The experimental points were obtained from the guarded cold plate measurements of Fig. 7. The lines are hemispherical emittances calculated from near-normal infrared reflectance measurements.

heat is removed from the metering piece at a precisely defined and stable rate. When there is no external heat flow into the metering piece, a primary null condition is established where dissipation of resistive power in the metering piece provides all of the heat that is removed. When there is external flow into the metering piece, a secondary null can be established at a lower value of resistive power dissipation in the metering piece. To a good approximation, the external heat flow is equal to the difference between the resistive power at the primary and secondary null conditions. Finite element modelling has been used to identify the magnitude of several systematic effects which result in small departures from this ideal behaviour. A metering piece has been constructed with an absorbing surface consisting of many black painted, small diameter, thin walled copper tubes. Measurements of the rate of radiative heat flow between two nominally identical surfaces can be used to calculate the emittance of this surface from the simple relationship for combining the hemispherical emittances of two grey surfaces. This emittance calculated in this way is 0.94 ± 0.01. Using this value, the emittances of uncoated and coated glass have been determined from measurements of radiative heat flow in the guarded cold plate apparatus. This emittance values so obtained agree to within the experimental error of approximately $\pm 5\%$ with those determined from infrared optical reflectance data.

Acknowledgements

This research was supported by His Royal Highness Prince Nawaf bin Abdul Aziz of the Kingdom of Saudi Arabia through the Science Foundation for Physics within The University of Sydney, and by the Australian Energy Research and Development Corporation through a post-graduate scholarship for C. J. Dey. We acknowledge with thanks contributions by H. Haldane, G. Mannes, J.-Z. Tang, and T. Pfeiffer.

References

[1] ASTM C 177-85. Standard test method for steady-state heat flux measurements and thermal transmission properties by means of the guarded-hot-plate apparatus. American Society for Testing and Materials, Philadelphia, PA, 1985.

[2] Collins RE, Davis CA, Dey CJ, Robinson SJ, Tang, J-Z, Turner GM. Measurement of local heat flow in flat evacuated glazing. International Journal of Heat and Mass Transfer 1993;36:2553–63.

[3] Büttner D, Fricke J, Krapf R, Reiss H. Measurement of thermal conductivity of evacuated load-bearing, high-temperature powder and glass board insulations with a 700×700 mm^2 guarded hot plate device. High Temperatures—High Pressures 1983;15:233–40.

[4] Shewen EC, Hollands KGT, Raithby GD. The measurement of surface heat flux using the Peltier effect. Journal of Heat Transfer 1989;111:798–803.

[5] Black IA, Glaser PE. The performance of a double-guarded cold-plate thermal conductivity apparatus. In Timmerhaus D, editor. Advances in Cryogenic Engineering, Vol. 9. New York: Plenum Press, 1964. pp. 52–63.

[6] Schmidt E, Wernerberg J. Wärmeflußmesser für hohe temperaturen. Zeitschrift des Vereines deutscher Ingenieure 1934;78:1–4.

[7] Zhang Q-C, Simko TM, Dey CJ, Collins RE, Turner GM, Brunotte M, Gombert A. The measurement and calculation of radiative heat transfer between uncoated and doped tin oxide coated glass surfaces. International Journal of Heat and Mass Transfer 1997;40:61–71.

[8] Dey CJ. Design and characterisation of novel thermal insulation materials. Ph.D. thesis, The University of Sydney, N.S.W., Australia, 1997.

[9] G+D Computing Pty Ltd. STRAND6 Finite Element Analysis System, Sydney, 1993.

[10] Pilkington K glass information sheet. Pilkington Glass Limited, U.K., 1989.

[11] Rubin M. Optical properties of soda lime silica glasses. Solar Energy Materials, 1985;12:275–88.